

Conversion of Dupin cyclide patches into rational biquadratic Bézier form

Sebti Foufou¹, Lionel Garnier¹, and Michael J. Pratt²

¹ LE2I, UMR CNRS 5158, UFR Sciences, Université de Bourgogne,
BP 47870, 21078 Dijon Cedex, France

`sfoufou@u-bourgogne.fr`, `lgarnier@u-bourgogne.fr`

² LMR Systems, 21 High Street, Carlton, Bedford, MK43 7LA, UK
`mike@lmr.clara.co.uk`

Abstract. This paper uses the symmetry properties of circles and Bernstein polynomials to establish a series of interesting *barycentric properties* of rational biquadratic Bézier patches. A robust algorithm is presented, based on these properties, for the conversion of Dupin cyclide patches into Bézier form. A set of conversion examples illustrates the use of this algorithm.

1 Introduction

Rational Biquadratic Bézier Surfaces (RBBSs) are tensor product parametric surfaces widely used in the first generation of computer graphics applications and geometric modelling systems. Good introductions to RBBSs may be found in [1–4].

Dupin cyclide surfaces represent a family of ringed surfaces, i.e., surfaces generated by a circle of variable radius sweeping through space [5–7]. It is possible to formulate them either as algebraic or parametric surfaces. In recent decades, the interest of several authors in these surfaces relates to their potential value in the development of CAGD tools [8, 9]. Also, cyclide intersections and the use of cyclides as blending surfaces have been investigated [10, 11].

The primary aim of this paper is to prove a series of useful properties of RBBSs, called *barycentric properties*, and to show how they can be used to convert cyclide patches into RBBSs. Section 2 gives background information concerning Rational Quadratic Bézier Curves (RQBCs) and RBBSs, introduces the Dupin cyclides, and discusses an algorithm for conversion of Dupin cyclide patches to RBBSs. Section 3 shows the use of RQBCs to represent circular arcs. Section 4 states and proves a set of new barycentric properties of RBBSs. Section 5 uses these properties to define a robust new algorithm for the conversion of Dupin cyclides into RBBSs, and illustrates some of the conversion results obtained. Section 6 presents our conclusions and suggests directions for future work.

2 Background

2.1 Rational quadratic Bézier curves and surfaces

A Rational Quadratic Bézier Curve (RQBC) is a second degree parametric curve defined by:

$$\overrightarrow{OM}(t) = \frac{1}{\sum_{i=0}^2 w_i B_i(t)} \left(\sum_{i=0}^2 w_i B_i(t) \overrightarrow{OP_i} \right), t \in [0, 1] \quad (1)$$

where $B_i(t)$ are quadratic Bernstein polynomials defined as: $B_0(t) = (1-t)^2$, $B_1(t) = 2t(1-t)$ and $B_2(t) = t^2$, and for $i \in \{0, 1, 2\}$, w_i are weights associated with the control points P_i . For a standard RQBC w_0 and w_2 are equal to 1, while w_1 can be used to control the type of conic defined by the curve.

Rational Biquadratic Bézier Surfaces (RBBSs) are defined by a tensor product of two RQBCs by:

$$\overrightarrow{OM}(u, v) = \frac{1}{\sum_{i=0}^2 \sum_{j=0}^2 w_{ij} B_i(u) B_j(v)} \sum_{i=0}^2 \sum_{j=0}^2 w_{ij} B_i(u) B_j(v) \overrightarrow{OP_{ij}} \quad (2)$$

More details on Bézier curves and surfaces can be found in [12, 4].

2.2 Dupin cyclides

Non-degenerate Dupin cyclides can be characterized by either of the following two equivalent implicit equations:

$$(x^2 + y^2 + z^2 - \mu^2 + b^2)^2 = 4(ax - c\mu)^2 + 4b^2 y^2 \quad (3)$$

$$(x^2 + y^2 + z^2 - \mu^2 - b^2)^2 = 4(cx - a\mu)^2 - 4b^2 z^2 \quad (4)$$

Parameters a , b and c are related by $c^2 = a^2 - b^2$. The parameter a is always greater than or equal to c . Parameters a , c and μ determine the type of the cyclide. When $c < \mu \leq a$ it is a ring cyclide, when $0 < \mu \leq c$ it is a horned cyclide, and when $\mu > a$ it is a spindle cyclide. The parametric form is represented by equation (5), where parameters θ and ψ satisfy $(0 \leq \theta, \psi \leq 2\pi)$:

$$\begin{cases} x(\theta, \psi) = \frac{\mu(c - a \cos \theta \cos \psi) + b^2 \cos \theta}{a - c \cos \theta \cos \psi} \\ y(\theta, \psi) = \frac{b \sin \theta \times (a - \mu \cos \psi)}{a - c \cos \theta \cos \psi} \\ z(\theta, \psi) = \frac{b \sin \psi \times (c \cos \theta - \mu)}{a - c \cos \theta \cos \psi} \end{cases} \quad (5)$$

These are the most important properties of Dupin cyclide surfaces:

- Simple mathematical representation in either implicit or parametric form.
- Circular lines of curvature. These lines of curvature correspond to isoparametric lines of constant θ or ψ . The angle between the surface normal and the principal normal on the lines of curvature is also constant.
- Each cyclide has two perpendicular planes of symmetry. The intersections of a cyclide with its planes of symmetry are two pairs of circles called the *principal circles*. These are the lines of curvature of the cyclide for which $\psi = 0$, $\psi = \pi$, $\theta = 0$ or $\theta = \pi$.
- In the parametric form, knowledge of the four principal circles allows the computation of the parameters a , c , and μ .
- The curvature line and tangent cone properties given above make it easy to use Dupin cyclides to create blends between other cyclide surfaces, including the important special cases of circular cylinders, circular cones, spheres and toruses.

2.3 Conversion of Dupin cyclides to RBBSs

If a RBBS is parameterized in terms of u and v , its isoparametric curves are conics. Lines of curvature of Dupin cyclides are circles, which are particular cases of conics. It is thus possible to convert a Dupin cyclide patch into an RBBS. In the rest of this paper, the Dupin cyclide patch to be converted will be referred to as a *cyclide patch*. It is assumed to be delimited by the curvature lines corresponding to parameter values $(\theta_0, \theta_1, \psi_0, \psi_1)$.

A conversion algorithm of the type discussed was proposed in [5]. The control points and their associated weights were determined from the parametric equation of the Dupin cyclide (equation (5)) by the following method:

1. The parameter transformations

$$\forall \theta \in \mathbb{R} - (\pi + 2\pi\mathbb{Z}), \quad \cos \theta = \frac{1 - \tan^2 U}{1 + \tan^2 U}, \quad \sin \theta = \frac{2 \tan U}{1 + \tan^2 U} \quad (6)$$

where $U = \tan(\theta/2)$, together with corresponding expressions for $\cos \psi$ and $\sin \psi$ in terms of $V = \tan(\psi/2)$, were used to obtain rational quadratic forms for the three coordinates in terms of U, V .

2. A linear reparametrization was now applied to obtain a representation in terms of u, v such that $u, v \in [0, 1]$.
3. The common denominator of the resulting scalar-valued rational biquadratics in u and v was reformulated in terms of the quadratic Bernstein basis functions. The resulting coefficients of those basis functions were identified with the weights w_{ij} in the denominator of equation (2).
4. Finally, with the weights known, the numerators of the three rational biquadratics were similarly reformulated. This gave the coordinates of the patch control points, expressed in terms of the defining constants of the particular cyclide, a, c, μ , together with the bounding parameter values of the original cyclide patch.

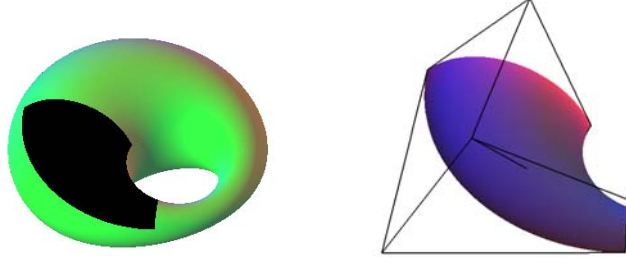


Fig. 1. Conversion of a Dupin cyclide patch (left) to RBBS (right) using Pratt's original algorithm.

Figure 1 shows an example of the conversion of a Dupin cyclide patch into a RBBS using this algorithm.

A problem with this algorithm is that the function \tan is discontinuous, not being defined for values $\frac{\pi}{2} + \pi\mathbb{Z}$. This has the results that

1. for certain choices of patch boundary the reparametrization functions are not defined (though these special cases could be identified and appropriate limiting values used);
2. more importantly, the algorithm gives incorrect results when $\pi \in]\theta_0, \theta_1[$ or when $\pi \in]\psi_0, \psi_1[$.

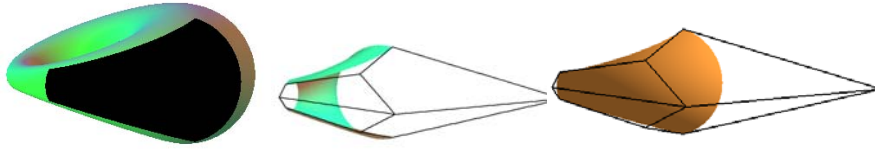


Fig. 2. Incorrect conversion. Left, the cyclide patch. Middle, the resulting RBBS representing the complementary patch, not the intended one. Right, the correct corresponding RBBS

Figure 2 illustrates a case of erroneous results from this algorithm. The cyclide patch (left subfigure) is defined by $a = 6$, $\mu = 3$, $c = 2$, $\theta_0 = \frac{\pi}{4}$, $\theta_1 = \frac{5\pi}{6}$, $\psi_0 = \frac{2\pi}{3}$ and $\psi_1 = \frac{4\pi}{3}$. To obtain the RBBS of the right subfigure, that correctly represents the cyclide patch of the left subfigure, we used a new variant of this algorithm obtained by taking the absolute value of the weights as calculated by Pratt's original formula, i.e.,

$$w_{ij} = |a(1 + G_i)(1 + H_j) - c(1 - G_i)(1 - H_j)| \quad (7)$$

In this formula, the variables G_i and H_j are intermediate values computed from \tan of $\theta_0/2$, $\theta_1/2$, $\psi_0/2$ and $\psi_1/2$ (see [5] for further details).

As we have seen, the boundary parameter values θ_0 , θ_1 , ψ_0 and ψ_1 , together with the values of a , c and μ , can be used to determine control points and weights of the RBBS. If $\theta_0 = 0$ and $\theta_1 = \frac{4\pi}{3}$, the computed control points calculated by the variant algorithm incorrectly correspond to the patch delimited by $\theta_0 = -\frac{2\pi}{3}$ and $\theta_1 = 0$. We must therefore require $|\theta_0 - \theta_1| < \pi$ and $|\psi_0 - \psi_1| < \pi$. Taking this constraint into consideration gives several possibilities for conversion of a complete Dupin cyclide. Figure 3 left illustrates a Dupin cyclide converted into 9 RBBSs using this new variant of the algorithm. Combined use of both the original and the variant algorithm allows to decrease the number of RBBSs to 6, which is believed to be the minimal number of RBBSs necessary for the representation of a complete Dupin cyclide (Figure 3 right). The new variant of



Fig. 3. Conversion of a whole Dupin cyclide into a set of RBBSs

this algorithm makes it possible to convert a whole Dupin cyclide into a set of RBBSs, but it is still not possible to convert a cyclide patch delimited by a curve obtained with one of the parameters equal to π . Moreover, having only positive weights is not enough to work correctly for certain cases where some control points need to have negative weights. Figure 4 shows a case where the original

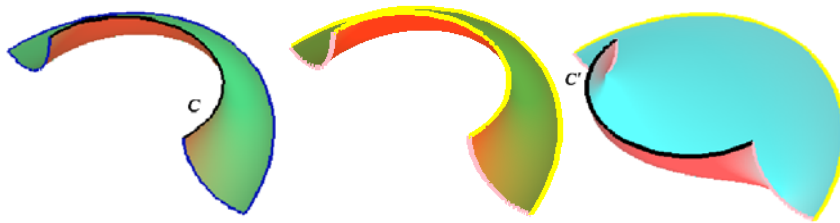


Fig. 4. Conversion of a cyclide patch. Left, the cyclide patch. Middle, the RBBS given by Pratt's algorithm. Right, the RBBS given by the variant of Pratt's algorithm.

algorithm works correctly (the middle subfigure) while the new variant fails (the right subfigure). The cyclide patch is defined by $a = 6$, $c = 2$, $\mu = 3$, $\theta_0 = -\frac{\pi}{3}$, $\theta_1 = \frac{\pi}{2}$, $\psi_0 = 0$ and $\psi_1 = \frac{\pi}{2}$. The output of the new variant is completely wrong: Border curve C' is the complement, on the circle, of the border curve C of the

cyclide patch. This is due to the fact that w_{10} is positive while it should be negative to model the border curve C . The same problem occurs for w_{11} . Another

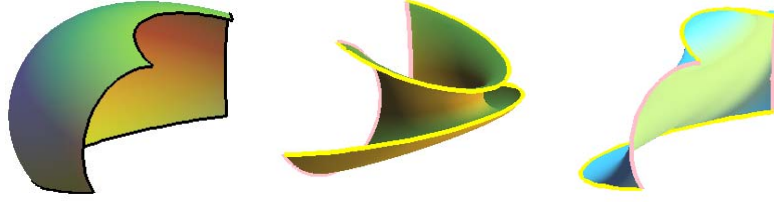


Fig. 5. A conversion example where both Pratt's algorithm and its variant fail.

conversion example is given in Figure 5. Parameters defining the cyclide patch are $a = 6$, $c = 2$, $\mu = 3$, $\theta_0 = \frac{2\pi}{3}$, $\theta_1 = \frac{4\pi}{3}$, $\psi_0 = \frac{5\pi}{6}$ and $\psi_1 = \frac{3\pi}{2}$. The original algorithm gives exactly the complement of the cyclide patch: the corner points are those of the cyclide patch while the delimiting curves are the complements, on the circle, of the curves defining the cyclide patch. On the other hand, the RBBS obtained by the new variant of this algorithm (right subfigure) has the same corner points and border curves as the cyclide patch, but the central control point P_{11} is not correct; the weight w_{11} should be negative, while the new variant gives only positive weights.

A less problematic conversion algorithm, based on barycentric properties of RBBSs and geometric properties of Dupin cyclides is proposed in section 5.

3 Modeling circular arcs using RQBCs

RQBCs can be used to model conics. Three control points and a scalar value (the weight of the middle control point) are enough to define an arc of a conic. In this section, we give some results on the expression of circular arcs using RQBC. Theorem 1 shows how to define a circle from two points and two tangents on these points. Theorem 2 presents how to compute the middle control point of the RQBC that represents a given circular arc. Theorem 3 shows how to compute the weight of the middle control point of the RQBC that represents a given circular arc. Figure 6 shows the modeling of circular arcs using RQBC. This is the geometric construction used for Theorems 1, 2 and 3. $\mathcal{C}(O_0, R)$ is a circle of centre O_0 and radius R . Segments $[P_0P_1]$ and $[P_2P_1]$ are tangents to the circle at points P_0 and P_2 . I_1 is the midpoint of segment $[P_0P_2]$. \mathcal{P} is the median plane of segment $[P_0P_2]$.

Theorem 1. *Circle from two points and tangents at these points.*

- If the circle $\mathcal{C}(O_0, R)$ exists then $P_1 \in \mathcal{P}$ and $P_1 \notin [P_0P_2]$. The radius is $R = O_0P_0$ and the centre O_0 is given by formula:

$$\overrightarrow{P_1O_0} = t_0 \overrightarrow{P_1I_1} \quad t_0 = \frac{P_0P_1^2}{I_1P_1 \bullet P_0P_1} \quad (8)$$

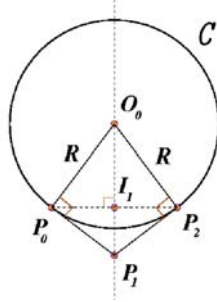


Fig. 6. Modeling circular arcs by RQBC

- In the plane determined by \mathcal{C} , the geometric angle $\widehat{P_0 O_0 P_2}$ is less than π , this means that if we take a parametrization γ of the circle in terms of cosine and sine such as $P_0 = \gamma(\theta_0)$, $P_2 = \gamma(\theta_1)$, we have $|\theta_0 - \theta_1| < \pi$.

Theorem 2. Computing control point P_1 when the centre of the circle is known. The RQBC is the arc of the circle \mathcal{C} passing through P_0 and P_2 . In this case, the control point P_1 satisfies:

$$\overrightarrow{I_1 P_1} = t_1 \overrightarrow{O_0 I_1} \quad t_1 = \frac{\overrightarrow{O_0 P_0} \bullet \overrightarrow{I_1 P_0}}{\overrightarrow{O_0 P_0} \bullet \overrightarrow{O_0 I_1}} \quad (9)$$

Theorem 3. Computing the weight w_1 .

The RQBC defined by control points P_0 , P_1 and P_2 and the weight w_1 is a circular arc if and only if the following condition hold:

$$|1 + w_1| R = |O_0 I_1 + w_1 O_0 P_1| \quad (10)$$

The RQBC defines the smaller arc of the circle if:

$$w_1 = \frac{O_0 I_1 - R}{R - O_0 P_1} = \frac{O_0 I_1 - O_0 P_0}{O_0 P_0 - O_0 P_1} > 0 \quad (11)$$

It defines the larger arc of the circle if:

$$w_1 = -\frac{O_0 I_1 + R}{R + O_0 P_1} = -\frac{O_0 I_1 + O_0 P_0}{O_0 P_0 + O_0 P_1} < 0 \quad (12)$$

Proofs of these three theorems can be easily obtained by combining properties of RQBC with those of the circle and scalar product.

4 Barycentric properties of RBBSs

Let S_0 be a Rational Biquadratic Bézier Surface (RBBS) defined according to formula (2) by control points $(P_{ij})_{0 \leq i, j \leq 2}$ and weights $(w_{ij})_{0 \leq i, j \leq 2}$ with $w_{00} =$

$w_{02} = w_{20} = w_{22} = 1$. In order to model surfaces with spherical curvatures by surface S_0 , we should have the following constraints on control points: P_{01} belongs to the median plane of $[P_{00}P_{02}]$, P_{10} belongs to the median plane of $[P_{00}P_{20}]$, P_{21} belongs to the median plane of $[P_{20}P_{22}]$ and P_{12} belongs to the median plane of $[P_{02}P_{22}]$.

The position of control point P_{11} is less obvious than the positions of the others. The following four theorems prove that P_{11} belongs to three particular lines. A set of interesting barycentric properties of RBBSs that helps in the construction of these lines are given and proved.

Theorem 4. *Let I_0, J_0, I_2 and J_2 be respectively the midpoints of the segments $[P_{00}P_{02}]$, $[P_{00}P_{20}]$, $[P_{20}P_{22}]$ and $[P_{02}P_{22}]$. We have the following four relations:*

$$\overrightarrow{OM\left(0, \frac{1}{2}\right)} = \frac{1}{1+w_{01}} \left(\overrightarrow{OI_0} + w_{01} \overrightarrow{OP_{01}} \right) \quad (13)$$

$$\overrightarrow{OM\left(1, \frac{1}{2}\right)} = \frac{1}{1+w_{21}} \left(\overrightarrow{OI_2} + w_{21} \overrightarrow{OP_{21}} \right)$$

$$\overrightarrow{OM\left(\frac{1}{2}, 0\right)} = \frac{1}{1+w_{10}} \left(\overrightarrow{OJ_0} + w_{10} \overrightarrow{OP_{10}} \right) \quad (14)$$

$$\overrightarrow{OM\left(\frac{1}{2}, 1\right)} = \frac{1}{1+w_{12}} \left(\overrightarrow{OJ_2} + w_{12} \overrightarrow{OP_{12}} \right)$$

Proof. In order to prove the result (13) for points $\overrightarrow{OM\left(0, \frac{1}{2}\right)}$ and $\overrightarrow{OM\left(1, \frac{1}{2}\right)}$, let us recall that $B_0(0) = 1, B_1(0) = B_2(0) = 0, B_2(1) = 1, B_1(1) = B_0(1) = 0, B_1\left(\frac{1}{2}\right) = \frac{1}{2}, B_0\left(\frac{1}{2}\right) = B_2\left(\frac{1}{2}\right) = \frac{1}{4}$, and if I is the midpoint of a segment $[AB]$, then for every point O we have $\overrightarrow{OA} + \overrightarrow{OB} = 2\overrightarrow{OI}$. By Formula (2), the point $\overrightarrow{OM\left(0, \frac{1}{2}\right)}$ on the RBBS is:

$$\begin{aligned} \overrightarrow{OM\left(0, \frac{1}{2}\right)} &= \frac{\sum_{i=0}^2 \sum_{j=0}^2 w_{ij} B_i(0) B_j\left(\frac{1}{2}\right) \overrightarrow{OP_{ij}}}{\sum_{i=0}^2 \sum_{j=0}^2 w_{ij} B_i(0) B_j\left(\frac{1}{2}\right)} = \frac{\sum_{j=0}^2 w_{0j} B_j\left(\frac{1}{2}\right) \overrightarrow{OP_{0j}}}{\sum_{j=0}^2 w_{0j} B_j\left(\frac{1}{2}\right)} \\ &= \frac{1}{\frac{w_{00}}{4} + \frac{w_{01}}{2} + \frac{w_{02}}{4}} \left(\frac{w_{00}}{4} \overrightarrow{OP_{00}} + \frac{w_{01}}{2} \overrightarrow{OP_{01}} + \frac{w_{02}}{4} \overrightarrow{OP_{02}} \right) \\ &= \frac{1}{\frac{1}{4} + \frac{w_{01}}{2} + \frac{1}{4}} \left(\frac{1}{4} \left(\overrightarrow{OP_{00}} + \overrightarrow{OP_{02}} \right) + \frac{w_{01}}{2} \overrightarrow{OP_{01}} \right) \\ &= \frac{1}{\frac{1}{2} + \frac{w_{01}}{2}} \left(\frac{1}{4} 2\overrightarrow{OI_0} + \frac{w_{01}}{2} \overrightarrow{OP_{01}} \right) \\ &= \frac{2}{1+w_{01}} \left(\frac{1}{2} \overrightarrow{OI_0} + \frac{1}{2} w_{01} \overrightarrow{OP_{01}} \right) \\ &= \frac{1}{1+w_{01}} \left(\overrightarrow{OI_0} + w_{01} \overrightarrow{OP_{01}} \right) \end{aligned}$$

On the other hand, point $\overrightarrow{OM\left(1, \frac{1}{2}\right)}$ on the RBBS is:

$$\begin{aligned}
\overrightarrow{OM\left(1, \frac{1}{2}\right)} &= \frac{\sum_{i=0}^2 \sum_{j=0}^2 w_{ij} B_i(1) B_j\left(\frac{1}{2}\right) \overrightarrow{OP_{ij}}}{\sum_{i=0}^2 \sum_{j=0}^2 w_{ij} B_i(1) B_j\left(\frac{1}{2}\right)} \\
&= \frac{1}{\sum_{j=0}^2 w_{2j} B_j\left(\frac{1}{2}\right)} \sum_{j=0}^2 w_{2j} B_j\left(\frac{1}{2}\right) \overrightarrow{OP_{2j}} \\
&= \frac{1}{\frac{w_{20}}{4} + \frac{w_{21}}{2} + \frac{w_{22}}{4}} \left(\frac{w_{20}}{4} \overrightarrow{OP_{20}} + \frac{w_{21}}{2} \overrightarrow{OP_{21}} + \frac{w_{22}}{4} \overrightarrow{OP_{22}} \right) \\
&= \frac{1}{\frac{1}{4} + \frac{w_{21}}{2} + \frac{1}{4}} \left(\frac{1}{4} (\overrightarrow{OP_{20}} + \overrightarrow{OP_{22}}) + \frac{w_{21}}{2} \overrightarrow{OP_{21}} \right) \\
&= \frac{1}{\frac{1}{2} + \frac{w_{21}}{2}} \left(\frac{1}{4} 2\overrightarrow{OI_2} + \frac{w_{21}}{2} \overrightarrow{OP_{21}} \right) \\
&= \frac{2}{1 + w_{21}} \left(\frac{1}{2} \overrightarrow{OI_2} + \frac{w_{21}}{2} \overrightarrow{OP_{21}} \right) = \frac{1}{1 + w_{21}} (\overrightarrow{OI_2} + w_{21} \overrightarrow{OP_{21}})
\end{aligned}$$

Result (14) of $\overrightarrow{OM\left(\frac{1}{2}, 0\right)}$ and $\overrightarrow{OM\left(\frac{1}{2}, 1\right)}$ can be proved in a similar way. \square

Theorem 5. Let G_0 be the isobarycentre of points $P_{00}, P_{02}, P_{20}, P_{22}$ and G_2 the barycentre of weighted points $(P_{10}, w_{10}), (P_{01}, w_{01}), (P_{12}, w_{12}), (P_{21}, w_{21})$. We define the value $w = w_{01} + w_{10} + w_{12} + w_{21}$ and G_1 as the barycentre of the weighted points $(G_0, 2)$ and (G_2, w) .

The point $M\left(\frac{1}{2}, \frac{1}{2}\right)$ satisfies the two following formulas:

$$\overrightarrow{OM\left(\frac{1}{2}, \frac{1}{2}\right)} = \frac{1}{2 + w + 2w_{11}} \left((2 + w) \overrightarrow{OG_1} + 2w_{11} \overrightarrow{OP_{11}} \right) \quad (15)$$

$$w_{11} \overrightarrow{M\left(\frac{1}{2}, \frac{1}{2}\right) P_{11}} = -\frac{2 + w}{2} \overrightarrow{M\left(\frac{1}{2}, \frac{1}{2}\right) G_1} \quad (16)$$

From the last formula we deduce that P_{11} belongs to the line $(M\left(\frac{1}{2}, \frac{1}{2}\right) G_1)$.

Proof. Evaluating equation (2) of the RBBSs at the point $\overrightarrow{OM\left(\frac{1}{2}, \frac{1}{2}\right)}$ gives:

$$\overrightarrow{OM\left(\frac{1}{2}, \frac{1}{2}\right)} = \frac{\sum_{i=0}^2 \sum_{j=0}^2 w_{ij} B_i\left(\frac{1}{2}\right) B_j\left(\frac{1}{2}\right) \overrightarrow{OP_{ij}}}{\sum_{i=0}^2 \sum_{j=0}^2 w_{ij} B_i\left(\frac{1}{2}\right) B_j\left(\frac{1}{2}\right)}$$

First, let us consider the denominator of this fraction:

$$\begin{aligned}
& \sum_{i=0}^2 \sum_{j=0}^2 w_{ij} B_i \left(\frac{1}{2} \right) B_j \left(\frac{1}{2} \right) = \sum_{i=0}^2 B_i \left(\frac{1}{2} \right) \left(\frac{w_{i0}}{4} + \frac{w_{i1}}{2} + \frac{w_{i2}}{4} \right) \\
&= \frac{\frac{w_{00}}{4} + \frac{w_{01}}{2} + \frac{w_{02}}{4}}{4} + \frac{\frac{w_{10}}{4} + \frac{w_{11}}{2} + \frac{w_{12}}{4}}{2} + \frac{\frac{w_{20}}{4} + \frac{w_{21}}{2} + \frac{w_{22}}{4}}{4} \\
&= \frac{\frac{w_{00}+w_{02}+w_{20}+w_{22}}{4} + \frac{w_{01}+w_{10}+w_{21}+w_{12}}{2} + \frac{w_{11}}{2}}{4} \\
&= \frac{w_{00} + w_{02} + w_{20} + w_{22}}{16} + \frac{w_{01} + w_{10} + w_{21} + w_{12}}{8} + \frac{w_{11}}{4} \\
&= \frac{2 + w + 2w_{11}}{8}
\end{aligned}$$

Second, the numerator can be similarly expressed as:

$$\begin{aligned}
& \sum_{i=0}^2 B_i \left(\frac{1}{2} \right) \left(\frac{w_{i0}}{4} \overrightarrow{OP_{i0}} + \frac{w_{i1}}{2} \overrightarrow{OP_{i1}} + \frac{w_{i2}}{4} \overrightarrow{OP_{i2}} \right) = \\
& \frac{w_{00}}{16} \overrightarrow{OP_{00}} + \frac{w_{01}}{8} \overrightarrow{OP_{01}} + \frac{w_{02}}{16} \overrightarrow{OP_{02}} + \frac{w_{10}}{8} \overrightarrow{OP_{10}} + \frac{w_{11}}{4} \overrightarrow{OP_{11}} + \\
& \frac{w_{12}}{8} \overrightarrow{OP_{12}} + \frac{w_{20}}{16} \overrightarrow{OP_{20}} + \frac{w_{21}}{8} \overrightarrow{OP_{21}} + \frac{w_{22}}{16} \overrightarrow{OP_{22}} \\
&= \left(\frac{1}{16} \overrightarrow{OP_{00}} + \frac{1}{16} \overrightarrow{OP_{02}} + \frac{1}{16} \overrightarrow{OP_{20}} + \frac{1}{16} \overrightarrow{OP_{22}} \right) + \\
& \left(\frac{w_{01}}{8} \overrightarrow{OP_{01}} + \frac{w_{10}}{8} \overrightarrow{OP_{10}} + \frac{w_{12}}{8} \overrightarrow{OP_{12}} + \frac{w_{21}}{8} \overrightarrow{OP_{21}} \right) + \frac{w_{11}}{4} \overrightarrow{OP_{11}} \\
&= \frac{1}{4} \overrightarrow{OG_0} + \frac{w}{8} \overrightarrow{OG_2} + \frac{w_{11}}{4} \overrightarrow{OP_{11}}
\end{aligned}$$

We may then write:

$$\begin{aligned}
\overrightarrow{OM \left(\frac{1}{2}, \frac{1}{2} \right)} &= \frac{1}{\frac{2+w+2w_{11}}{8}} \left(\frac{1}{4} \overrightarrow{OG_0} + \frac{w}{8} \overrightarrow{OG_2} + \frac{w_{11}}{4} \overrightarrow{OP_{11}} \right) \\
&= \frac{8}{2+w+2w_{11}} \left(\frac{1}{4} \overrightarrow{OG_0} + \frac{w}{8} \overrightarrow{OG_2} + \frac{w_{11}}{4} \overrightarrow{OP_{11}} \right) \\
&= \frac{1}{2+w+2w_{11}} \left(2\overrightarrow{OG_0} + w\overrightarrow{OG_2} + 2w_{11}\overrightarrow{OP_{11}} \right) \\
&= \frac{1}{2+w+2w_{11}} \left((2+w)\overrightarrow{OG_1} + 2w_{11}\overrightarrow{OP_{11}} \right)
\end{aligned}$$

which proves the result (15). This latter is valid for any point O so it is valid for the point $M \left(\frac{1}{2}, \frac{1}{2} \right)$. Hence, substituting O by $M \left(\frac{1}{2}, \frac{1}{2} \right)$ in (15) gives:

$$\begin{aligned}
(2+w+2w_{11}) \overrightarrow{M \left(\frac{1}{2}, \frac{1}{2} \right) M \left(\frac{1}{2}, \frac{1}{2} \right)} &= \\
& \overrightarrow{(2+w) M \left(\frac{1}{2}, \frac{1}{2} \right) G_1 + 2w_{11} M \left(\frac{1}{2}, \frac{1}{2} \right) P_{11}}
\end{aligned}$$

Consequently, we have: $\vec{0} = (2 + w) \overrightarrow{M\left(\frac{1}{2}, \frac{1}{2}\right)G_1} + 2w_{11} \overrightarrow{M\left(\frac{1}{2}, \frac{1}{2}\right)P_{11}}$. Hence:

$$w_{11} \overrightarrow{M\left(\frac{1}{2}, \frac{1}{2}\right)P_{11}} = -\frac{2 + w}{2} \overrightarrow{M\left(\frac{1}{2}, \frac{1}{2}\right)G_1}$$

□

Theorem 6. Let G_3 be the barycentre of weighted points $(P_{00}, 9)$, $(P_{20}, 9)$, $(P_{02}, 1)$, $(P_{22}, 1)$, $(P_{01}, 6w_{01})$, $(P_{21}, 6w_{21})$, $(P_{10}, 18w_{10})$, $(P_{12}, 2w_{12})$, and $W_1 = 20 + 6w_{01} + 18w_{10} + 2w_{12} + 6w_{21}$.

The point $M\left(\frac{1}{2}, \frac{1}{4}\right)$ satisfies the two following formulas:

$$\overrightarrow{OM\left(\frac{1}{2}, \frac{1}{4}\right)} = \frac{1}{W_1 + 12w_{11}} \left(W_1 \overrightarrow{OG_3} + 12w_{11} \overrightarrow{OP_{11}} \right) \quad (17)$$

$$(W_1 + 12w_{11}) \overrightarrow{G_3M\left(\frac{1}{2}, \frac{1}{4}\right)} = 12w_{11} \overrightarrow{G_3P_{11}} \quad (18)$$

From the last formula we deduce that P_{11} belongs to the line $(G_3M\left(\frac{1}{2}, \frac{1}{4}\right))$.

Proof. Before starting the proof of result (17) for point $\overrightarrow{OM\left(\frac{1}{2}, \frac{1}{4}\right)}$, recall that $B_0\left(\frac{1}{4}\right) = \frac{9}{16}$, $B_1\left(\frac{1}{4}\right) = \frac{3}{8}$ and $B_2\left(\frac{1}{4}\right) = \frac{1}{16}$. By formula (2) we have:

$$\overrightarrow{OM\left(\frac{1}{2}, \frac{1}{4}\right)} = \frac{1}{\sum_{i=0}^2 \sum_{j=0}^2 w_{ij} B_i\left(\frac{1}{2}\right) B_j\left(\frac{1}{4}\right)} \sum_{i=0}^2 \sum_{j=0}^2 w_{ij} B_i\left(\frac{1}{2}\right) B_j\left(\frac{1}{4}\right) \overrightarrow{OP_{ij}}$$

The denominator can be easily reduced to:

$$\begin{aligned} & \sum_{i=0}^2 \sum_{j=0}^2 w_{ij} B_i\left(\frac{1}{2}\right) B_j\left(\frac{1}{4}\right) = \sum_{i=0}^2 B_i\left(\frac{1}{2}\right) \left(\frac{9w_{i0}}{16} + \frac{6w_{i1}}{16} + \frac{w_{i2}}{16} \right) \\ &= \frac{9w_{00} + 9w_{20} + w_{02} + w_{22} + 6w_{01} + 6w_{21} + 18w_{10} + w_{12} + 12w_{11}}{64} \\ &= \frac{20 + 6w_{01} + 6w_{21} + 18w_{10} + w_{12} + 12w_{11}}{64} \\ &= \frac{W_1 + 12w_{11}}{64} \end{aligned}$$

Using this result and expanding the numerator gives the required proof:

$$\begin{aligned} \overrightarrow{OM\left(\frac{1}{2}, \frac{1}{4}\right)} &= \frac{64}{W_1 + 12w_{11}} \left(\frac{9}{64} \overrightarrow{OP_{00}} + \frac{6w_{01}}{64} \overrightarrow{OP_{01}} + \frac{w_{02}}{64} \overrightarrow{OP_{02}} \right) + \\ & \frac{64}{W_1 + 12w_{11}} \left(\frac{18}{64} \overrightarrow{OP_{10}} + \frac{12w_{11}}{64} \overrightarrow{OP_{11}} + \frac{2w_{02}}{64} \overrightarrow{OP_{12}} \right) + \\ & \frac{64}{W_1 + 12w_{11}} \left(\frac{9}{64} \overrightarrow{OP_{20}} + \frac{6w_{21}}{64} \overrightarrow{OP_{21}} + \frac{1}{64} \overrightarrow{OP_{22}} \right) \\ &= \frac{1}{W_1 + 12w_{11}} \left(W_1 \overrightarrow{OG_3} + 12w_{11} \overrightarrow{OP_{11}} \right) \end{aligned}$$

From these results we deduce:

$$(W_1 + 12w_{11}) \overrightarrow{G_3 M \left(\frac{1}{2}, \frac{1}{4} \right)} = 12w_{11} \overrightarrow{G_3 P_{11}}$$

which is the result (18)

□

Theorem 7. Let G_4 be the barycentre of weighted points $(P_{00}, 9)$, $(P_{20}, 1)$, $(P_{02}, 9)$, $(P_{22}, 1)$, $(P_{10}, 6w_{10})$, $(P_{12}, 6w_{12})$, $(P_{01}, 18w_{01})$, $(P_{21}, 2w_{21})$, and $W_2 = 20 + 6w_{10} + 18w_{01} + 2w_{21} + 6w_{12}$.

The point $M \left(\frac{1}{4}, \frac{1}{2} \right)$ satisfies the two following formulas:

$$\overrightarrow{OM \left(\frac{1}{4}, \frac{1}{2} \right)} = \frac{1}{W_2 + 12w_{11}} \left(W_2 \overrightarrow{OG_4} + 12w_{11} \overrightarrow{OP_{11}} \right) \quad (19)$$

$$(W_2 + 12w_{11}) \overrightarrow{G_4 M \left(\frac{1}{4}, \frac{1}{2} \right)} = 12w_{11} \overrightarrow{G_4 P_{11}} \quad (20)$$

From the last formula we deduce that P_{11} belongs to the line $(G_4 M \left(\frac{1}{4}, \frac{1}{2} \right))$.

Proof. The results (19) and (20) can be proved in the same way as (17) and (18) or (15) and (16). □

5 A new Dupin cyclide to RBBS conversion algorithm

In this section we propose a new algorithm (Algorithm 1) for converting a Dupin cyclide patch or a whole Dupin cyclide into RBBS form. The algorithm is based on the barycentric properties of RBBSs given by the theorems of Sections 3 and 4.

The goal is to develop a conversion method that exploits and keeps circular symmetries along the isoparametric curves of Dupin cyclides. These latter are not surfaces of revolution, so, in step six of this algorithm, we have to be sure that lines $(G_1 \Gamma(\theta_2, \psi_2))$, $(G_3 \Gamma(\theta_2, \psi_3))$ and $(G_4 \Gamma(\theta_3, \psi_2))$ have the same point of intersection. This is true provided that θ_0 and θ_1 (or ψ_0 and ψ_1) are symmetrical compared to 0 or π on the trigonometric circle.

A set of conversion examples is presented in the following sections.

Algorithm 1

Given: A Dupin cyclide defined by a parametric map Γ , and a patch on this cyclide delimited by parameter values: $\theta_0, \theta_1, \psi_0$ and ψ_1 with $|\theta_0 - \theta_1| < \pi$ and $|\psi_0 - \psi_1| < \pi$. These values also define four (circular) curvature lines on the Dupin cyclide

Find: The representation of this patch as a RBBS S over $[0, 1] \times [0, 1]$, defined by nine control points P_{ij} and nine weights w_{ij} , $0 \leq i, j < 2$. Weights w_{ij} will be equal to one except $w_{10}, w_{01}, w_{21}, w_{12}$ and w_{11} , which can be either positive or negative.

Procedure:

1. Obtain corner control points directly by: $P_{00} = \Gamma(\theta_0, \psi_0)$, $P_{02} = \Gamma(\theta_1, \psi_0)$, $P_{20} = \Gamma(\theta_0, \psi_1)$, $P_{22} = \Gamma(\theta_1, \psi_1)$.
2. Find centres of the four circles of curvature using a point on each line of curvature.
3. Find control points P_{01} , P_{10} , P_{12} and P_{21} on the median planes of curvature lines using equation (9) of Theorem 2.
4. Calculate weights w_{10} , w_{01} , w_{21} and w_{12} using equations (11) or (12) of Theorem 3.
5. Consider two RQBC γ_u and γ_v defined on the borders of the region to be converted. Control points and the weight of γ_u are P_{00} , P_{10} , P_{20} and w_{10} . Those of γ_v are P_{00} , P_{01} , P_{02} and w_{01} .
 - Find θ_2 and θ_3 solutions of equations $\gamma_u(\frac{1}{2}) = \Gamma(\theta_2, \psi_0)$ and $\gamma_u(\frac{1}{4}) = \Gamma(\theta_3, \psi_0)$.
 - Find ψ_2 and ψ_3 solutions of equations $\gamma_v(\frac{1}{2}) = \Gamma(\theta_0, \psi_2)$ and $\gamma_v(\frac{1}{4}) = \Gamma(\theta_0, \psi_3)$.
6. Compute the last control point P_{11} as the intersection of lines $(G_1\Gamma(\theta_2, \psi_2))$ and $(G_3\Gamma(\theta_2, \psi_3))$. Constructions of G_1 and G_3 are given in Theorems 5 and 6.
7. Compute weight w_{11} , using equation (16) of Theorem 7

5.1 Conversion examples

Figure 7 illustrates the conversions of two Dupin cyclide patches into RBBSs using the proposed algorithm. For the first example (the upper subfigures), we obtained a standard RBBS having only positive weights. For the second one (the lower subfigures), in which the cyclide patch is delimited by $\psi_1 = \pi$, we obtained a RBBS with positive and negative weights. These are positive along curvature lines with θ constant, and negative along curvature lines with ψ constant.

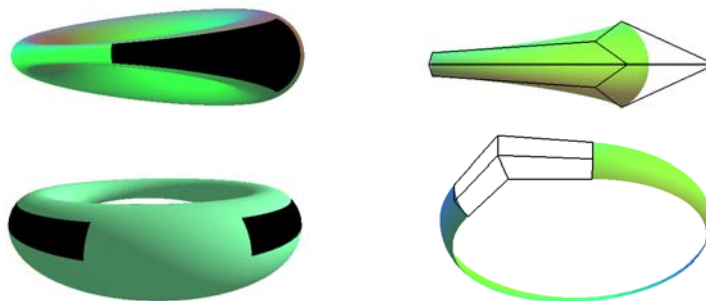


Fig. 7. Conversion of two cyclide patches into RBBSs. Upper, the result is a standard RBBS having only positive weights. Lower, the result is a RBBS with positive and negative weights

5.2 Comparison of conversion algorithms

To make a significant comparison of the various algorithms for converting Dupin cyclides to RBBS form (Pratt's original algorithm, the new variant of the Pratt's algorithm and the barycentric algorithm), we have used the following criteria:

- Entire cyclide: whether it is possible or not to convert a whole Dupin cyclide into a set of RBBSs.
- Number of RBBSs: The minimum number of RBBSs needed to represent a whole Dupin cyclide.
- Parameter constraints: what are the constraints on parameters θ_0 , θ_1 , ψ_0 and ψ_1 ?
- Prohibited values: Are there particular prohibited values for parameters θ_0 , θ_1 , ψ_0 and ψ_1 ?

	Pratt's algorithm	Variant of Pratt's algorithm	Barycentric algorithm
Entire cyclide	no	yes	yes
Number of RBBSs	/	9	4
Geometric constraints	no	$\begin{cases} \theta_0 - \theta_1 < \pi \\ \psi_0 - \psi_1 < \pi \end{cases}$	(θ_0, θ_1) or (ψ_0, ψ_1) symmetrical compared to 0 or π .
Prohibited value	π	π	no

Table 1. Comparison between Pratt's algorithm, its variant and the barycentric algorithm.

Table 1 summarizes this comparison. One can note that to convert a whole Dupin cyclide we need: Only four RBBSs if the new algorithm is used, nine RBBSs if the Pratt's algorithm is used, and six RBBSs if the Pratt's algorithm and its variant are combined and used. Figure 8 shows this difference in the number of resulting RBBSs.

Dupin cyclides are very useful for blending quadric surfaces [8, 13–15]. To show conversion of a blending Dupin cyclide we applied the method proposed in [8] to construct the blending cyclide of the left subfigure of Figure 9 and converted it to RBBSs by the three conversion algorithms discussed in this paper. We note here that conversion showed in the middle subfigure can be obtained either by the new algorithm or by a combination of Pratt's algorithm and its variant; two RBBSs are enough to ensure a correct conversion. On the other hand, Pratt's algorithm gives conversion showed on the right subfigure. Although in this case, the minimal number of RBBSs is three, the surfaces obtained here have only positive weights so they lie completely inside their control polyhedron.

Another case where the new algorithm is better than both of others is shown by Figure 10. The cyclide patch (left subfigure) is the one of Figure 5 where Pratt's

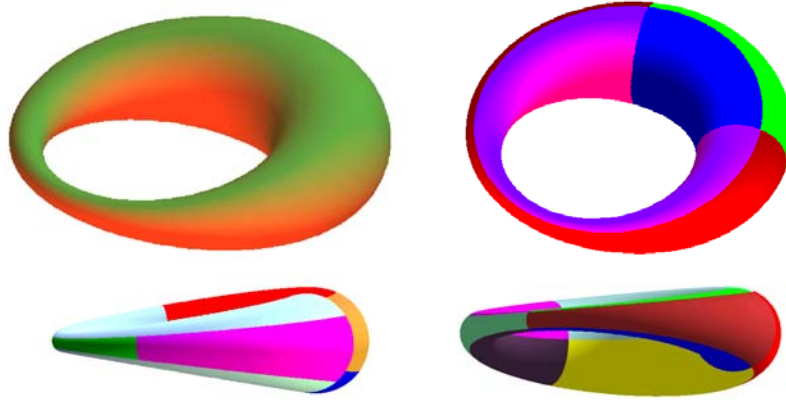


Fig. 8. Comparison of conversion algorithms. Upper left, the cyclide to be converted. Upper right, result of the new algorithm: only four RBBSs are necessary. Lower left, result of the combination of Pratt’s algorithm and its variant, six RBBSs are necessary. Lower right, result of the variant of Pratt’s algorithm, nine RBBSs are necessary.

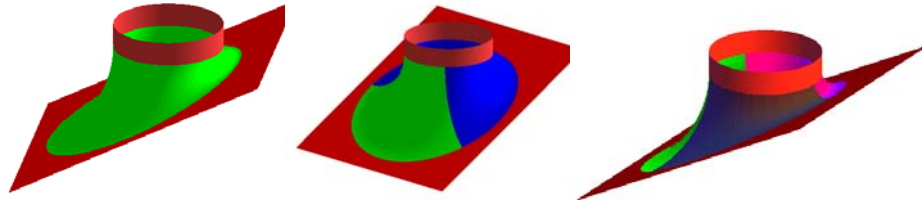


Fig. 9. Conversion of cylinder/plane blending Dupin cyclide. Left, the blending cyclide. Middle, conversion into two RBBSs. Right, conversion into three RBBSs

algorithm and its variant have given incorrect conversions. The new algorithm exactly reproduces the original cyclide patch (Figure 10 right).

Another advantage of the new algorithm is the possibility of converting a Dupin cyclide patch delimited by a curvature line corresponding to a parameter value of π , which is not feasible either with Pratt’s algorithm or its variant. This is shown in Figure 11 where the cyclide patch to be converted is a blending surface of a cylinder and a plane. Horizontally, it is delimited, on the cylinder side by $\psi_1 = \frac{\pi}{2}$ and on the plane side by $\psi_0 = \pi$. Neither Pratt’s algorithm nor its variant can be used to achieve this conversion. Two samples of possible conversions, using the barycentric algorithm, are given on subfigures 11 middle and 11 right.

5.3 A complete case study

As control points of RBBSs resulting from conversion may be far removed from the patches themselves, it is often difficult to draw the control polygon on figures that show these RBBSs. So, in this section we give more details concerning the

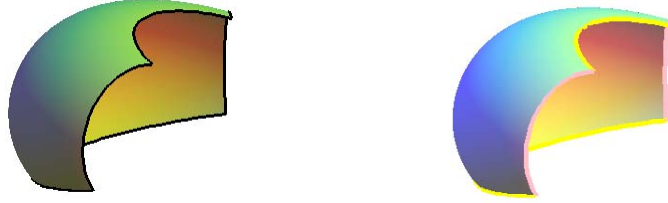


Fig. 10. Another conversion result. The new algorithm gives exact conversion (right subfigure), while other algorithms fail (see Figure 5.)

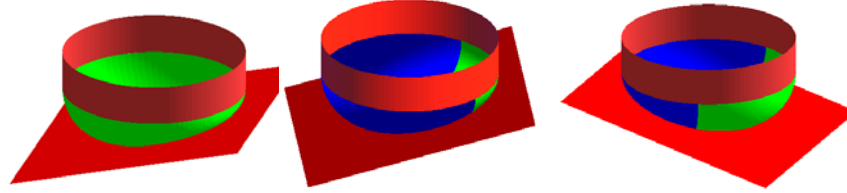


Fig. 11. Conversion of cylinder/plane blending Dupin cyclide where neither Pratt's algorithm nor its variant can be applied. Left, the blending cyclide. Middle and right, two examples of possible conversions

conversion of the cyclide patch of Figure 5 left, and the RBBSs given by the conversion algorithms. Parameters defining the cyclide patch are $a = 6$, $c = 2$, $\mu = 3$, $\theta_0 = \frac{2\pi}{3}$, $\theta_1 = \frac{4\pi}{3}$, $\psi_0 = \frac{5\pi}{6}$ and $\psi_1 = \frac{3\pi}{2}$. Table 2 gives control points and weights of RBBSs of Figure 5 middle and Figure 10 right. This table shows how computed control points differ from one algorithm to another. A value of 1 is an exact value, whereas a value of 48.000 is a rounded of value. The only difference between Pratt's algorithm and its variant is the fact that negative weights become positive. On the other hand, weights computed using our algorithm are smaller than those given by Pratt's algorithm; moreover, the new algorithm gives exact values for corner control points, unlike the other algorithms.

[Points;Weights]	Pratt's algorithm	barycentric algorithm
$[P_{00}; w_{00}] \simeq$	$[(-3.466; 8.206; -2.204); 306.564]$	$[(-3.466; 8.206; -2.204); 1]$
$[P_{01}; w_{01}] \simeq$	$[(-5.995; 12.852; 5.302); -46.641]$	$[(-5.995; 12.852; 5.302); 0.384]$
$[P_{02}; w_{02}] \simeq$	$[(-1.667; 4.899; 3.771); 48.000]$	$[(-1.667; 4.899; 3.771); 1]$
$[P_{10}; w_{10}] \simeq$	$[(-35.166; -0.191; -7.807); -75.713]$	$[(-35.166; -0.422; -7.807); 0.247]$
$[P_{11}; w_{11}] \simeq$	$[(129.663; 0.682; -42.661); -5.072]$	$[(129.663; 0; -42.661); -0.042]$
$[P_{12}; w_{12}] \simeq$	$[(-9.667; -0.566; 6.600); -24.000]$	$[(-9.667; -0.117; 6.600); 0.500]$
$[P_{20}; w_{20}] \simeq$	$[(-3.466; -8.205; -2.204); 306.564]$	$[(-3.466; -8.205; -2.204); 1]$
$[P_{21}; w_{21}] \simeq$	$[(-5.995; -12.852; 5.302); -46.641]$	$[(-5.995; -12.852; 5.302); 0.384]$
$[P_{22}; w_{22}] \simeq$	$[(-1.667; -4.899; 3.771); 48.000]$	$[(-1.667; -4.899; 3.771); 1]$

Table 2. Comparison of control points obtained with Pratt's algorithm and barycentric algorithm.

6 Conclusion

In this paper, we have used the symmetry properties of circles and Bernstein polynomials to prove seven theorems concerning barycentric properties of RBBSs. These properties have been employed in a new algorithm for the conversion of Dupin cyclides to RBBSs. Several examples of the use of the algorithm have been given.

In future it is proposed to extend the algorithm for the conversion of supercyclides (affine or projective transformations of Dupin cyclides) to RBBSs.

References

1. Piegl, L., Tiller, W.: A menagerie of rational B-spline circles. *IEEE Computer Graphics and Applications* **9** (1989) 46–56
2. Forrest, A.R.: *Curves and Surfaces for Computer-Aided Design*. PhD thesis, University of Cambridge, UK (1968)
3. Demengel, G., Pouget, J.: *Mathématiques des Courbes et des Surfaces: Modèles de Bézier, des B-Splines et des NURBS*. Volume 1. Ellipse (1998)
4. Hoschek, J., Lasser, D.: *Fundamentals of Computer Aided Geometric Design*. A.K.Peters, Wellesley, MA. (1993)
5. Pratt, M.J.: Cyclides in computer aided geometric design. *Computer Aided Geometric Design* **7** (1990) 221–242
6. Chandru, V., Dutta, D., Hoffmann, C.M.: Variable radius blending using Dupin cyclides. In Wozny, M., Turner, J.U., Preiss, K., eds.: *Geometric Modelling for Product Engineering*, North-Holland Publ. Co. (1990) (Proc. IFIP/NSF Workshop on Geometric Modelling, Rensselaerville, NY, Sept 1988).
7. Degen, W.L.F.: Generalized cyclides for use in CAGD. In Bowyer, A., ed.: *Computer-Aided Surface Geometry and Design*, Oxford University Press (1994) 349–363 (Proc. 4th IMA Conference on the Mathematics of Surfaces, Bath, UK, Sept. 1990).
8. Pratt, M.J.: Cyclides in computer aided geometric design II. *Computer Aided Geometric Design* **12** (1995) 131–152
9. Dutta, D., Martin, R.R., Pratt, M.J.: Cyclides in surface and solid modeling. *IEEE Computer Graphics and Applications* **13** (1993) 53–59
10. Paluszny, M., Boehm, W.: General cyclides. *Computer Aided Geometric Design* **15** (1998) 699–710
11. Shene, C.: Blending two cones with Dupin cyclides. *Computer Aided Geometric Design* **15** (1998) 643–673
12. Farin, G.: *Curves And Surfaces*. 3 edn. Academic Press (1993)
13. Aumann, G.: Curvature continuous connections of cones and cylinders. *Computer-aided Design* **27** (1995) 293–301
14. Shene, C.: Do blending and offsetting commute for Dupin cyclides? *Computer Aided Geometric Design* **17** (2000) 891–910
15. Wallner, J., Pottmann, H.: Rational blending surfaces between quadrics. *Computer Aided Geometric Design* **14** (1997) 407–419